Experimental evaluation of ecological principles to understand and modulate the outcome of bacterial strain competition in gut microbiomes

Rafael R. Segura Munoz
University of Nebraska-Lincoln
Sara Mantz
University of Nebraska-Lincoln
Ines Martinez
University of Alberta
Robert J. Schmaltz
University of Nebraska-Lincoln
Jens Walter (jenswalter@ucc.ie)
APC Microbiome Ireland; University College Cork
Amanda E. Ramer-Tait (aramer-tait2@unl.edu)
University of Nebraska-Lincoln

Research Article

Keywords: Microbiome, niche, competitive exclusion, coexistence theory, gut ecosystems, engraftment, live biotherapeutics, intraspecific interactions, priority effects

Posted Date: December 8th, 2020

DOI: https://doi.org/10.21203/rs.3.rs-123088/v1

Version of Record: A version of this preprint was published at The ISME Journal on February 24th, 2022.
See the published version at https://doi.org/10.1038/s41396-022-01208-9.

Abstract

It is unclear if coexistence theory can be applied to gut microbiomes to understand their characteristics and modulate their composition. Through strictly controlled colonization experiments in mice, we demonstrated that strains of *Akkermansia muciniphila* and *Bacteroides vulgatus* could only be established if microbiomes were devoid of exactly these species. Strains of *A. muciniphila* showed strict competitive exclusion, while *B. vulgates* strains coexistedbut populations were still influenced by competitive interactions. Priority effects were detected for both species as strains' competitive fitness increased when colonizing first. Based on these observations, we devised a subtractive strategy for *A. muciniphila* using antibiotics and demonstrated that a strain from an assembled community can be stably replaced by another strain. Altogether, these results suggest that aspects of coexistence theory, e.g., niche partitioning and the impact of priority effects on fitness differences, can be applied to explain ecological characteristics of gut microbiomes and modulate their composition.

Introduction

The gut microbiota is considered an important aspect of host health, influencing digestion, immune system development and pathogen invasion (Buffie et al., 2015; Schubert et al., 2015; Brugiroux et al., 2016; He et al., 2017; Ma et al., 2019; Vivarelli et al., 2019; Rodriguez et al., 2020). Moreover, numerous studies have documented differences in microbiome composition and function between healthy and diseased humans and animals (Walters et al., 2014; Pasolli et al., 2016). Strategies aimed at modulating and restoring the ecological and physiological features of the gut microbiome have therefore gained much momentum (Sonnenburg et al., 2016; Rastelli et al., 2018). Considering the complexity of the gut ecosystem, successful modulation of gut microbiomes is likely to require the application of ecological theory (Costello et al., 2012; Walter and Ley, 2011;Koskella et al., 2017).

The introduction of live microbes, either as single strains (e.g., probiotics, live biotherapeutics) or complex mixtures (e.g., fecal microbiota transplants), into the gut ecosystem represents one approach to modifying the microbiome. However, the ecological conditions required for sustained long-term colonization (i.e., engraftment) of orally administered live microbial products are poorly understood (Walter et al., 2018). Recent evidence suggests that engraftment may depend on the pre-treatment microbiome composition, especially the absence of closely related species (Maldonado-Gómez et al., 2016; Martínez et al., 2018; Smillie et al., 2018; Le Roy et al., 2019). We (Maldonado-Gómez et al., 2016; Martínez et al., 2018) and others (Low et al., 2012; Seekatz et al., 2014; Li et al., 2016; Smillie et al., 2018; Le Roy et al., 2019) have shown that the resident microbiome influences engraftment of incoming species, likely through competitive exclusion where newly-arriving species cannot coexist with established species if they occupy exactly the same niche (and are competing for identical resources) (Hardin, 1960). In particular, Maldonado and colleagues showed that persistence of the probiotic *Bifidobacterium longum* AH1206 in select study participants was associated with low abundance of *B. longum* species (Maldonado-Gómez et al., 2016). Lack of colonization in other participants may thus be explained by competitive exclusion (Hardin, 1960). However, these findings are based on associations

and it has not established if competitive exclusion is in fact the causative factor that determines engraftment. Indeed, not all outcomes from microbiome-based interventions are consistent with competitive exclusion and instead indicated coexistence of related strains in fecal transplants (Stecher et al., 2010; Li et al., 2016; Smillie et al., 2018). These discrepancies illustrate that the ecological factors governing engraftment are complex, insufficiently understood, and likely extend beyond the competitive exclusion principle (Koskella et al., 2017).

Modern coexistence theory suggests that competitive exclusion and coexistence are determined by equalizing mechanisms, which are influenced by fitness differences among species and stabilizing mechanisms (i.e., niche differences through resource partitioning) that alter the balance between interspecific and intraspecific competition (Chesson, 2000; Grainger et al., 2019). Competitive interactions are further historically contingent, meaning that order of arrival of a species into an ecosystem can result in priority effects that alter the outcome of species interactions, e.g., by benefiting early colonizers over late colonizers (Grainger et al., 2019). For gut ecosystems, competitive exclusion has been demonstrated for isogenic bacterial strains orally administered to germ-free mice (Onderdonk et al., 1981; Lee et al., 2013). However, such an experiment represents an extreme condition where the competing strains are essentially identical and have maximum niche overlap. Strains in natural communities possess genetic and trait variation and strains used as live microbial products are likely to differ from resident microbiota members. To what degree contemporary niche and coexistence theory applies to interactions among members of the gut microbiota and the introduction of microbes into gut microbiomes has not been experimentally tested.

Here, we performed systematic experiments in gnotobiotic mice to test the applicability of coexistence theory to the stable establishment of gut microbes and to determine if such information can be utilized to stably modulate the gut microbiota at the strain level. We selected two species of gut bacteria, *Akkermansia muciniphila* and *Bacteroides vulgatus*, based on their importance in modulating host metabolism (Everard et al., 2013; Shin et al., 2014) and immunity (Png et al., 2010; Dingemanse et al., 2015; Zhai et al., 2019). To study niche occupancy and intraspecific competition under close-to-natural but strictly controlled conditions, we utilized gnotobiotic mice colonized with complex microbiomes with and without *A. muciniphila* and *B. vulgatus*. We specifically tested (i) to what degree the absence of a species determines colonization, (ii) if colonization can be prevented or altered by prior introduction of another strain of a species, and (iii) the effect of colonization order on coexistence between strains of the same species. Finally, we applied the information gained from these experiments to design a subtractive antibiotic strategy with the aim of removing an *A. muciniphila* strain from an assembled community and replacing it with a different strain.

Results

A. muciniphila and *B. vulgatus* strains only colonized gnotobiotic mice harboring complex microbiomes devoid of exactly these species.

To confirm published studies showing that bacterial colonization in the mammalian gut depends on the absence of related bacteria (Lee et al., 2013; Maldonado-Gómez et al., 2016; Obadia et al., 2017; Martínez et al., 2018), we introduced *A. muciniphila* and *B. vulgatus* strains into mice harboring complex microbiomes with (positive) and without (negative) these species (confirmed by 16S rRNA gene sequencing and species-specific qPCR) and compared persistence over five weeks using strain-specific qPCR (Figure 1A). Neither *A. muciniphila* nor *B. vulgatus* strains colonized mice carrying a microbiome that contained these species (Figure 1B and C). In contrast, stable persistence was achieved in mice devoid of *A. muciniphila* and *B. vulgatus* at the beginning of the study (Figure 1D and E). Together, these results demonstrate that colonization of exogenous bacterial strains can occur in the absence, but not presence, of the same species in the resident microbiome, thus confirming similar previous findings in both mice and humans (Maldonado-Gómez et al., 2016; Martínez et al., 2018).

Colonization of *A. muciniphila*, but not *B. vulgatus*, was strictly governed by competitive exclusion and priority effects.

The findings above suggest that concepts such as competitive exclusion or limiting similarity pertain to gut ecosystems (Meszéna et al., 2006). To experimentally test the importance of these concepts for bacterial colonization in the mammalian gut, we colonized germ-free mice with a “permissive” negative microbiome devoid of *A. muciniphila* and *B. vulgatus* and a mixture of both *A. muciniphila* BAA-835 and *B. vulgatus* 8482. Two weeks later, mice were colonized with a mixture of both *A. muciniphila* YL44 and *B. vulgatus* RJ2H1 (Figure 2A). A second cohort of mice harboring permissive microbiomes were colonized with both *A. muciniphila* YL44 and *B. vulgatus* RJ2H1 first, followed by *A. muciniphila* BAA-835 and *B. vulgatus* 8482 two weeks later (Figure 2B). Finally, a third cohort of mice colonized with the permissive microbiome was used to test all four strains together to determine fitness differences of the strains (Figure 2C).

For *A. muciniphila*, we observed that the strain arriving first stably colonized, while the second was only temporarily detected, indicating competitive exclusion (Figure 2D and E). Notably, competition outcomes were strictly dependent on arrival order, with the first colonizer excluding the later colonizer, thus demonstrating that priority effects are of paramount importance. Priority effects were also strong enough to abrogate the fitness differences observed between the two *A. muciniphila* strains. Strain BAA-835 completely outcompeted YL44 when it colonized first, although it was outcompeted by YL44 when both strains were inoculated together (Figure 2F).

In contrast to the findings obtained for *A. muciniphila*, both strains of *B. vulgatus* were able to stably colonize independently of strain arrival succession (Figure 2E, H, and I). Despite stable coexistence, the two strains still influenced one another’s abundance, indicating competitive interactions that were further influenced by priority effects. First, the maximum abundance levels for both strains were significantly higher (mean estimate of difference 0.5-1.0 log, $p<0.05$) when they colonized first as compared to when

colonizing second (Figure 2G versus H). Second, the higher population level of strain RJ2H1 (~10^8 cells/g feces) compared to 8482 (~10^6 cells/g feces) observed when RJ2H1 colonized first or at the same time as 8482 was no longer detectable when strain 8482 was introduced first (both strains at ~10^7 cells/g feces). These findings indicate that although the two *B. vulgatus* strains coexisted and were not subjected to strict competitive exclusion, the two strains still affected each other's population levels and priority effects clearly influenced competition outcomes.

Strain-to-strain differences in traits enabling niche differentiation may explain the distinct competition outcomes between *A. muciniphila* and *B. vulgatus* strains.

Similarities between bacteria increase competition for resources and may result in competitive exclusion (Cavender-Bares et al., 2009). However, differences in resource requirements can lead to resource partitioning and niche differentiation and thus constitute a stabilizing mechanism that increases the chance of coexistence (Chesson, 2000). We therefore sought to investigate whether genetic relationships could explain the differences in coexistence patterns observed between *A. muciniphila* (strict competitive exclusion) and *B. vulgatus* (coexistence with competitive interactions) strains. An assessment of genetic relatedness using genome-wide average nucleotide identity (gANI) and alignment fraction (AF) metrics (Varghese et al., 2015) revealed that the genomes of the two *A. muciniphila* strains were more similar to one another than those of the *B. vulgatus* strains (gANI values of 99.10 versus 98.68 and AF values of 93.37 versus 75.58 for *A. muciniphila* and *B. vulgatus* strain, respectively; Table 1). We also observed that the genomes of *A. muciniphila* strains were smaller than those of *B. vulgatus* strains (Figure 3A) and consistent in size with organisms exhibiting specialist behaviors such as mucin degradation/utilization (Tramontano et al., 2018). Each *A. muciniphila* strain differed from one another in only a few unique encoded proteins related to processes of gene regulation and nitrogen metabolism (Figure 3B and D). In contrast, the *B. vulgatus* strains differed by multiple proteins related to processes of gene regulation, carbohydrate binding and metabolism, phage infection, stress responses, and protein degradation (Figure 3C and E). These findings suggest that competitive exclusion between *A. muciniphila* strains is likely related to high genetic similarity whereas coexistence of *B. vulgatus* strains may be determined by unique genes, especially those involved in carbohydrate metabolism, which may confer the ability to utilize different resources and thus promote niche differentiation.

A subtractive antibiotic strategy enabled replacement of an established *A. muciniphila* strain.

Our observations for *A. muciniphila* suggest that the establishment of a new strain of this species is prevented through competitive exclusion by a resident strain of the same species whose fitness is enhanced through priority effects. This finding provides a mechanism underlying the difficulty in establishing new strains within the gut microbiota and implies that successful colonization of novel *A. muciniphila* strains depends upon the reduction or removal of a pre-existing, related strain within the

microbiome using a subtractive approach (Walter et al., 2018). One potential strategy for such modulation is antibiotic treatment (Walker et al., 2013). We therefore hypothesized that an antibiotic regimen would allow us to replace an established strain of *A. muciniphila* with a novel strain. We selected candidate antibiotics based on Derrien et. al., who reported that *A. muciniphila* was susceptible to ampicillin (AMP) (Derrien et al., 2004) and other reports describing antibiotics with effects on *A. muciniphila* or Verrucomicrobia (Pérez-Cobas et al., 2013; Dingemanse et al., 2015; Livanos et al., 2016). Candidate antibiotics were first screened *in vitro* for their ability to attenuate growth of *A. muciniphila* BAA-835 and YL44 (Table 2). Macrolide tylosin tartrate (MTT), clarithromycin (CLA), and AMP all limited the growth of BAA and YL44 *in vitro*.

To test the feasibility of an antibiotic-based subtractive strategy, germ-free mice were first conventionalized with a permissive microbiota devoid of *A. muciniphila* and then colonized one week later with strain BAA-835. One week after the addition of BAA-835, mice received either CLA, MTT, AMP, AMP + MTT, AMP + MTT + CLA, or no antibiotics in their drinking water for five days. On the fifth day, mice receiving antibiotics were returned to regular drinking water and began receiving daily gavages of YL44 for five days (Figure 4A). In agreement with findings from our previous experiment, YL44 was only transiently detectible in control mice and did not influence BAA-835 population levels (Figure 4B). Treatment with either MTT or CLA resulted in the same outcomes as observed for control mice (Figure 4C and D). In contrast, administering AMP alone or in combination with MTT and/or CLA depleted the existing BAA strain to undetectable levels and enabled stable colonization of YL44 for the duration of the five-week experiment (Figure 4E-G). Together, these results demonstrate that subtractive antibiotic treatment can be used as a strategy to successfully remove a pre-existing *A. muciniphila* strain from an assembled gut microbial community and replace it with a novel strain that would otherwise be excluded by competitive exclusion. These experiments also further confirm that the competitive interactions between *A. muciniphila* strains detected in previous experiments are not due to interactions with *B. vulgatus*.

Discussion

Recent studies suggest that colonization resistance in a microbiome is determined by the presence of closely related species (Lee et al., 2013; Maldonado-Gómez et al., 2016; Obadia et al., 2017; Martínez et al., 2018), thus suggesting that principles such as competitive exclusion apply to gut ecosystems. However, the applicability of these concepts has not been empirically established, nor have there been attempts to apply them to exchange strains in an assembled community. Using systematic experiments in gnotobiotic mice, we found that *A. muciniphila* strains, which have narrow niches, excluded one another from the microbiome whereas *B. vulgatus* strains could coexist, likely through niche partitioning, but still showed ecological interactions pointing to competition. We observed that competitive interactions between both *A. muciniphila* and *B. vulgatus* strains were influenced by time of arrival, thus establishing the importance of priority effects as a determinant of coexistence. Finally, we demonstrated that antibiotic treatments can be used to replace *A. muciniphila* strains within a complex microbiome. Altogether, our results suggest that important aspects of coexistence theory, e.g., the ability to partition

niches and the impact of priority effects on fitness differences, determine strain competition outcomes in gut ecosystems and suggest that such principles can be applied to design strategies that modulate microbiomes.

According to modern coexistence theory, coexistence in an ecosystem is determined by the degree to which members differ in fitness (equalizing mechanisms), their niches (stabilizing mechanisms), and their time of arrival (Chesson, 2000; Adler et al., 2007; Levine et al., 2009; Grainger et al., 2019). Our findings agree with these principles, which can provide an explanation for the profound differences between *A. muciniphila* and *B. vulgatus* with respect to coexistence. *A. muciniphila* colonizes the mucus layer (Everard et al., 2013), an anatomically-defined structure composed primarily of mucin agglomerates (Forstner, 1995), and preferentially metabolizes mucin over other carbohydrates (Derrien et al., 2004; Ottman et al., 2017), thus restricting the variability of resources in its ecological niche. These behaviors are also consistent with the small genomic differences between strains BAA-835 and YL44, indicating that these strains are ecologically very similar. Consequently, one would predict that stabilizing mechanisms are reduced between competing *A. muciniphila* strains because they are unable to partition niches, which should result in strict competitive exclusion where the better competitor excludes the other strain. These assumptions are supported by our current observations for *A. muciniphila*. However, our findings indicate that the ability of these strains to compete (fitness) is influenced by arrival order. Specifically, the less fit *A. muciniphila* strain actually won the competition when it arrived first. Our results therefore confirm the importance of priority effects in gut ecosystems (Martínez et al., 2018) and demonstrate that these effects can be strong enough to overcome inherent fitness differences between *A. muciniphila* strains.

Unlike *A. muciniphila* strains, *B. vulgatus* strains do not exclude each other. This observation can be explained by the existence of stabilizing mechanisms that lead to niche differentiation. In contrast to *A. muciniphila,* whose niche is restricted to the mucus layer, *B. vulgatus* colonizes food particles and scattered luminal regions adjacent to the colonic mucosa (Mark et al., 2017; Whitaker et al., 2017). The *B. vulgatus* niche is therefore likely much more complex and dynamic than that of *A. muciniphila* and provides a larger range of substrates that become accessible by different strains. Indeed, the larger genomes for *B. vulgatus* compared to *A. muciniphila* suggest that these strains are generalists (Walter and Ley., 2011). Consistently, *B. vulgatus* strains 8482 and RJ2H1 also differed in diversity of carbohydrate and protein degradation capabilities and substrate binding, which suggests that they are able to partition niches and stably coexist even if equalizing mechanisms are low due to fitness differences (Chesson, 2000). Despite the stable coexistence of *B. vulgatus* strains, we still detected competitive interactions that were influenced by priority effects. *B. vulgatus* strains achieved a higher colonization level when they arrived first, and fitness differences could be overcome through early arrival. Overall, our observations for *B. vulgatus* strains are consistent with coexistence theory in that strains capable of partitioning niches can coexist. However, our experiments have not identified the environmental conditions that allow niche differentiation within *B. vulgatus*, and we do know why incoming strains were excluded from a microbiome when that species was already present (may indicate that several related strains had previously secured complete occupancy of the niches that *B. vulgatus* can

partition). Future mechanistic studies to experimentally determine the mechanisms of niche partitioning within *B. vulgatus* are therefore required. Regardless of the exact mechanisms, a novel and important finding for our understanding of the gut ecosystem is that even if strains stably coexist, their population levels are still affected by competition and influenced by priority effects.

Taken together, our findings suggest that key aspects of modern coexistence theory can be applied to understand fundamental characteristics of gut microbial communities. In accordance with that theory, species and strains with similar fitness levels can coexist when niche differences are sufficiently large to reduce overlap in resource usage (Chesson, 2000). In contrast, if niches overlap too much, then fitness differences prevent coexistence and result in competitive exclusion (Chesson, 2000). Our observations for *A. muciniphila* provide experimental evidence to support previous findings that point to competitive exclusion as a mechanism for colonization resistance (Lee et al., 2013; Maldonado-Gómez et al., 2016; Obadia et al., 2017; Martínez et al., 2018). Importantly, we demonstrate that priority effects can be strong enough to modify and even reverse fitness differences between strains and consequently alter competition outcomes, regardless of whether they result in strict competitive exclusion or coexistence. Our current results extend our previous findings that priority effects can influence the persistence of individual colonizers and the historical contingency of microbiome assembly (Martinez et al., 2018) by providing evidence for how arrival order shapes fitness differences among strains and ultimately the outcome of their competition. Priority effects, in the context of modern coexistence theory, can therefore provide mechanistic explanations for key characteristics of gut ecosystems. First, competitive exclusion, in combination with priority effects, provides a mechanism that enhances colonization resistance of gut microbiomes as it endows the established organism with a fitness advantage over later arrivals, thereby providing an explanation for microbiome stability, resistance, and resilience (Faith et al., 2013; Mehta et al., 2018). Second, priority effects could explain why maternal-derived bacteria, which are likely to arrive early, are more stable colonizers compared to non-maternal strains (Ferretti et al., 2018; Korpela et al., 2018). Third, priority effects can influence the abundance of coexisting community members, thus offering a mechanism by which arrival order (which is likely to be largely stochastic) creates differences in gut microbiota composition and explains, in part, the substantial interindividual variation observed in gut microbiomes (Martínez et al., 2018).

Considering these ecological concepts, there are substantial practical implications for successfully introducing a new strain into the gut microbiota: (i) closely-related established strains must be absent (Maldonado-Gómez et al., 2016; Segura Munoz et al., 2020), (ii) the incoming strain (which is disadvantaged by priority effects) must outcompete the resident strain, or (iii) the resident strain currently occupying the niche must first be removed through subtractive approaches. The third strategy has been both proposed and applied in some fecal microbiota transplant studies (Ji et al., 2017; Walter et al., 2018; Freitag et al., 2019), but it is unclear if it constitutes a mechanism to improve engraftment. Our findings demonstrated that a subtractive approach based on antibiotic treatment could indeed be used to replace an established *A. muciniphila* strain with a new one. Specifically, administration of antibiotics suppressed the abundance of the competing, early-arriving *A. muciniphila* strain and opened a niche for the late-arriving strain to colonize. Subtractive approaches such as antibiotics may therefore enable microbiome

modulation by both suppressing competing strains and opening niches for new colonizers. We acknowledge that the use of broad-spectrum antibiotics such as ampicillin to replace strains has substantial disadvantages for translation into humans. More targeted subtractive methods, including the use of bacteriophages (Divya Ganeshan et al., 2019) or CRISPR/cas systems (Ramachandran et al., 2019), are likely more desirable, and, if applied in agreement with ecological theory, could pave the way for precision tools to modulate microbiomes. Importantly, our study provides the proof-of-concept that such approaches can be successful.

In conclusion, this study demonstrates the applicability of the central aspects of modern coexistence theory to gut ecosystems and that such theory can be used to understand engraftment of incoming microbes. Our findings provide potential explanations for many fundamental characteristics of the gut microbiome, including stability, colonization resistance, enhanced stability of maternally-acquired strains, and drivers of inter-subject variation. Furthermore, this work informs future intervention studies aimed at modulating gut ecosystems using live microbes, which will likely need to be personalized based on an individual's baseline microbiome and attempt to remove competitors through subtractive approaches. Admittedly, our study only tested two strains each of two important bacterial species, and the ecological principles governing other microbiota members and the context in which they apply, might differ. Future research should extend our work to other species and ideally combine gnotobiotic models of disease with genetic studies to identify the exact mechanisms by which microbes coexist in gut ecosystems and how their relationships are influenced by pathologies that alter the gut microbiota.

Declarations

Acknowledgments

This work was supported by a Young Investigator Grant in Probiotics from the Global Probiotics Council to A.E.R.T. J.W. is funded in part by Science Foundation Ireland Centre grant to APC Microbiome Ireland (APC/SFI/12/RC/2273_P2). We thank the staff of the Nebraska Gnotobiotic Mouse Program for their technical expertise and skillful animal husbandry. We also thank Dr. Daniel Peterson for kindly providing *B. vulgatus* RJ2H1 for our experiments. The funders had no role in the study design, data collection and analysis, decision to publish, or preparation of the manuscript.

Author Contributions

Conceptualization: J.W. and A.E.R.T; Investigation: R.R.S.M. and S.M.; Methodology: R.R.S.M., R.J.S., J.W. and A.E.R.T.; Resources: A.E.R.T., J.W. and I.M.; Writing: R.R.S.M, J.W. and A.E.R.T; Funding Acquisition: A.E.R.T.

Declaration of Interests

The authors declare no conflict of interest pertaining to this project.

Competing interests

The authors declare no competing interests.

References

Adler, P. B., Hillerislambers, J. and Levine, J. M. (2007). A niche for neutrality. Ecol. Lett. *10*, 95–104.

Bindels, L. B., Segura Munoz, R. R., Gomes-Neto, J. C., Mutemberezi, V., Martínez, I., Salazar, N., Cody, E. A., Quintero-Villegas, M. I., Kittana, H., de los Reyes-Gavilán, C. G., et al. (2017). Resistant starch can improve insulin sensitivity independently of the gut microbiota. Microbiome *5*, 1–16.

Brown, D. F. and Kothari, D. (1975). Comparison of antibiotic discs from different sources. J. Clin. Pathol. *28*, 779–783.

Brugiroux, S., Beutler, M., Pfann, C., Garzetti, D., Ruscheweyh, H.-J., Ring, D., Diehl, M., Herp, S., Lötscher, Y., Hussain, S., et al. (2016). Genome-guided design of a defined mouse microbiota that confers colonization resistance against *Salmonella enterica* serovar Typhimurium. Nat. Microbiol. *2*, 16215.

Buffie, C. G., Bucci, V., Stein, R. R., McKenney, P. T., Ling, L., Gobourne, A., No, D., Liu, H., Kinnebrew, M., Viale, A., et al. (2015). Precision microbiome reconstitution restores bile acid mediated resistance to *Clostridium difficile*. Nature *517*, 205–208.

Cavender-Bares, J., Kozak, K. H., Fine, P. V. A. and Kembel, S. W. (2009). The merging of community ecology and phylogenetic biology. Ecol. Lett. *12*, 693–715.

Chen, I.-M. A., Chu, K., Palaniappan, K., Pillay, M., Ratner, A., Huang, J., Huntemann, M., Varghese, N., White, J. R., Seshadri, R., et al. (2019). IMG/M v.5.0: an integrated data management and comparative analysis system for microbial genomes and microbiomes. Nucleic Acids Res. *47*, 666–677.

Chesson, P. (2000). Mechanisms of maintenance of species diversity. Annu. Rev. Ecol. Syst. *31*, 343–366.

Consortium, U. (2008). The universal protein resource (UniProt). Nucleic Acids Res. *36*, D190–D195.

Costello, E. K., Stagaman, K., Dethlefsen, L., Bohannan, B. J. M. and Relman, D. A. (2012). The application of ecological theory toward an understanding of the human microbiome. Science *336*, 1255–1262.

Derrien, M., Vaughan, E. E., Plugge, C. M. and de Vos, W. M. (2004). Akkermansia muciniphila gen. nov., sp. nov., a human intestinal mucin-degrading bacterium. Int. J. Syst. Evol. Microbiol. *54*, 1469–1476.

Dingemanse, C., Belzer, C., van Hijum, S. A. F. T., Günthel, M., Salvatori, D., den Dunnen, J. T., Kuijper, E. J., Devilee, P., de Vos, W. M., van Ommen, G. B., et al. (2015). *Akkermansia muciniphila* and *Helicobacter typhlonius* modulate intestinal tumor development in mice. Carcinogenesis *36*, 1388–1396.

Divya Ganeshan, S. and Hosseinidoust, Z. (2019). Phage therapy with a focus on the human microbiota. Antibiotics *8*, 131.

El-Gebali, S., Mistry, J., Bateman, A., Eddy, S. R., Luciani, A., Potter, S. C., Qureshi, M., Richardson, L. J., Salazar, G. A., Smart, A., et al. (2019). The Pfam protein families database in 2019. Nucleic Acids Res. *47*, 427–432.

Everard, A., Belzer, C., Geurts, L., Ouwerkerk, J. P., Druart, C., Bindels, L. B. and Guiot, Y. (2013). Cross-talk between *Akkermansia muciniphila* and intestinal epithelium controls diet-induced obesity. Proc. Natl. Acad. Sci. *110*, 9066–71.

Faith, J. J., Guruge, J. L., Charbonneau, M., Subramanian, S., Seedorf, H., Goodman, A. L., Clemente, J. C., Knight, R., Heath, A. C., Leibel, R. L., et al. (2013). The long-term stability of the human gut microbiota. Science *341*, 1237439.

Ferretti, P., Pasolli, E., Tett, A., Asnicar, F., Gorfer, V., Fedi, S., Armanini, F., Truong, D. T., Manara, S., Zolfo, M., et al. (2018). Mother-to-infant microbial transmission from different body sites shapes the developing infant gut microbiome. Cell Host Microbe *24*, 133–145.

Forstner, G. (1995). Signal Transduction Packaging and Secretion of Mucins. Annu. Rev. Physiol. *57*, 585–605.

Freitag, T. L., Hartikainen, A., Jouhten, H., Sahl, C., Meri, S., Anttila, V.-J., Mattila, E., Arkkila, P., Jalanka, J. and Satokari, R. (2019). Minor effect of antibiotic pre-treatment on the engraftment of donor microbiota in fecal transplantation in mice. Front. Microbiol. *10*, 2685.

Gomes-Neto, J. C., Kittana, H., Mantz, S., Segura Munoz, R. R., Schmaltz, R. J., Bindels, L. B., Clarke, J., Hostetter, J. M., Benson, A. K., Walter, J., et al. (2017). A gut pathobiont synergizes with the microbiota to instigate inflammatory disease marked by immunoreactivity against other symbionts but not itself. Sci. Rep. *7*, 17707.

Gomes-Neto, J. C., Mantz, S., Held, K., Sinha, R., Segura Munoz, R. R., Schmaltz, R., Benson, A. K., Walter, J. and Ramer-Tait, A. E. (2017). A real-time PCR assay for accurate quantification of the individual members of the Altered Schaedler Flora microbiota in gnotobiotic mice. J. Microbiol. Methods *135*, 52–62.

Grainger, T. N., Letten, A. D., Gilbert, B. and Fukami, T. (2019). Applying modern coexistence theory to priority effects. Proc. Natl. Acad. Sci. *116*, 6205–6210.

Hardin, G. (1960). The competitive exclusion principle. Science *131*, 1292–1297.

He, M. and Shi, B. (2017). Gut microbiota as a potential target of metabolic syndrome: the role of probiotics and prebiotics. Cell Biosci. *7*, 54.

Ji, S. K., Yan, H., Jiang, T., Guo, C. Y., Liu, J. J., Dong, S. Z., Yang, K. L., Wang, Y. J., Cao, Z. J. and Li, S. L. (2017). Preparing the gut with antibiotics enhances gut microbiota reprogramming efficiency by promoting xenomicrobiota colonization. Front. Microbiol. *8*, 1208.

Korpela, K., Costea, P., Coelho, L. P., Kandels-Lewis, S., Willemsen, G., Boomsma, D. I., Segata, N. and Bork, P. (2018). Selective maternal seeding and environment shape the human gut microbiome. Genome Res. *28*, 561–568.

Koskella, B., Hall, L. J. and Metcalf, C. J. E. (2017). The microbiome beyond the horizon of ecological and evolutionary theory. Nat. Ecol. Evol. *1*, 1606–1615.

Lagkouvardos, I., Pukall, R., Abt, B., Foesel, B. U., Meier-Kolthoff, J. P., Kumar, N., Bresciani, A., Martínez, I., Just, S., Ziegler, C., et al. (2016). The mouse intestinal bacterial collection (miBC) provides host-specific insight into cultured diversity and functional potential of the gut microbiota. Nat. Microbiol. *1*, 16131.

Lee, S. M., Donaldson, G. P., Mikulski, Z., Boyajian, S., Ley, K. and Mazmanian, S. K. (2013). Bacterial colonization factors control specificity and stability of the gut microbiota. Nature *501*, 426–429.

Levine, J. M. and HilleRisLambers, J. (2009). The importance of niches for the maintenance of species diversity. Nature *461*, 254–257.

Li, S. S., Zhu, A., Benes, V., Costea, P. I., Hercog, R., Hildebrand, F., Huerta-Cepas, J., Nieuwdorp, M., Salojärvi, J., Voigt, A. Y., et al. (2016). Durable coexistence of donor and recipient strains after fecal microbiota transplantation. Science *352*, 586–589.

Livanos, A. E., Greiner, T. U., Vangay, P., Pathmasiri, W., Stewart, D., McRitchie, S., Li, H., Chung, J., Sohn, J., Kim, S., et al. (2016). Antibiotic-mediated gut microbiome perturbation accelerates development of type 1 diabetes in mice. Nat. Microbiol. *1*, 16140.

Low, D. E., Shahinas, D., Silverman, M., Sittler, T., Chiu, C., Kim, P., Allen-Vercoe, E., Weese, S., Wong, A. and Pillaij, D. R. (2012). Toward an understanding of changes in diversity associated with fecal microbiome transplantation based on 16s rRNA gene deep sequencing. MBio *3*, 1–10.

Ma, W., Mao, Q., Xia, W., Dong, G., Yu, C. and Jiang, F. (2019). Gut microbiota shapes the efficiency of cancer therapy. Front. Microbiol. *10*, 1050.

Maldonado-Gómez, M. X., Martínez, I., Bottacini, F., O'Callaghan, A., Ventura, M., van Sinderen, D., Hillmann, B., Vangay, P., Knights, D., Hutkins, R. W., et al. (2016). Stable engraftment of *Bifidobacterium longum* AH1206 in the human gut depends on individualized features of the resident microbiome. Cell Host Microbe *20*, 515–526.

Mark, J. L., Hasegawa, Y., Mcnulty, N. P., Gordon, J. I. and Borisy, G. G. (2017). Spatial organization of a model 15-member human gut microbiota established in gnotobiotic mice. Proc. Natl. Acad. Sci. *114*, 9105–9114.

Martínez, I., Maldonado-Gomez, M. X., Gomes-Neto, J. C., Kittana, H., Ding, H., Schmaltz, R., Joglekar, P., Cardona, R. J., Marsteller, N. L., Kembel, S. W., et al. (2018). Experimental evaluation of the importance of colonization history in early-life gut microbiota assembly. Elife *7*, e36521.

Mavromatis, K., Chu, K., Ivanova, N., Hooper, S. D., Markowitz, V. M. and Kyrpides, N. C. (2009). Gene context analysis in the integrated microbial genomes (IMG) data management system. PLoS One *4*, e7979–e7979.

Mehta, R. S., Abu-Ali, G. S., Drew, D. A., Lloyd-Price, J., Subramanian, A., Lochhead, P., Joshi, A. D., Ivey, K. L., Khalili, H., Brown, G. T., et al. (2018). Stability of the human faecal microbiome in a cohort of adult men. Nat. Microbiol. *3*, 347–355.

Meszéna, G., Gyllenberg, M., Pásztor, L. and Metz, J. A. J. (2006). Competitive exclusion and limiting similarity: A unified theory. Theor. Popul. Biol. *69*, 68–87.

Mukherjee, S., Stamatis, D., Bertsch, J., Ovchinnikova, G., Katta, H. Y., Mojica, A., Chen, I.-M. A., Kyrpides, N. C. and Reddy, T. B. K. (2018). Genomes online database (GOLD) v.7: updates and new features. Nucleic Acids Res. *47*, 649–659.

Obadia, B., Güvener, Z. T., Zhang, V., Ceja-Navarro, J. A., Brodie, E. L., Ja, W. W. and Ludington, W. B. (2017). Probabilistic invasion underlies natural gut microbiome stability. Curr. Biol. *27*, 1999–2006.

Onderdonk, A., Marshall, B. and Cisneros, R. (1981). Competition between congenic *Escherichia coli* K-12 strains in vivo *32*, 74–79.

Ottman, N., Davids, M., Suarez-Diez, M., Boeren, S., Schaap, P. J., Martins dos Santos, V. A. P., Smidt, H., Belzer, C. and de Vos, W. M. (2017). Genome-scale model and omics analysis of metabolic capacities of *Akkermansia muciniphila* reveal a preferential mucin-degrading lifestyle. Appl. Environ. Microbiol. Edited by R. M. Kelly *83*, e01014-17.

Pasolli, E., Truong, D. T., Malik, F., Waldron, L. and Segata, N. (2016). Machine learning meta-analysis of large metagenomic datasets: Tools and biological insights. PLOS Comput. Biol. *12*, e1004977.

Pérez-Cobas, A. E., Gosalbes, M. J., Friedrichs, A., Knecht, H., Artacho, A., Eismann, K., Otto, W., Rojo, D., Bargiela, R., von Bergen, M., et al. (2013). Gut microbiota disturbance during antibiotic therapy: a multi-omic approach. Gut *62*, 1591–1601.

Png, C. W., Lindén, S. K., Gilshenan, K. S., Zoetendal, E. G., McSweeney, C. S., Sly, L. I., McGuckin, M. A. and Florin, T. H. J. (2010). Mucolytic bacteria with increased prevalence in IBD mucosa augment in vitro utilization of mucin by other bacteria. Am. J. Gastroenterol. *105*, 2420–2428.

Ramachandran, G. and Bikard, D. (2019). Editing the microbiome the CRISPR way. Philos. Trans. R. Soc. Lond. B. Biol. Sci. *374*, 20180103.

Rastelli, M., Knauf, C. and Cani, P. D. (2018). Gut microbes and health: A focus on the mechanisms linking microbes, obesity, and related disorders. Obesity (Silver Spring). *26*, 792–800.

Rodriguez, J., Hiel, S., Neyrinck, A. M., Le Roy, T., Pötgens, S. A., Leyrolle, Q., Pachikian, B. D., Gianfrancesco, M. A., Cani, P. D., Paquot, N., et al. (2020). Discovery of the gut microbial signature driving the efficacy of prebiotic intervention in obese patients. Gut *0*, 1–13.

Le Roy, T., Debédat, J., Marquet, F., Da-Cunha, C., Ichou, F., Guerre-Millo, M., Kapel, N., Aron-Wisnewsky, J. and Clément, K. (2019). Comparative evaluation of microbiota engraftment following fecal microbiota transfer in mice models: Age, kinetic and microbial status matter. Front. Microbiol. *10*, 1–16.

Rozen, S. and Skaletsky, H. (2000). Primer3 on the WWW for general users and for biologist programmers. Methods Mol. Biol. *132*, 365–386.

Schneeberger, M., Everard, A., Gómez-Valadés, A. G., Matamoros, S., Ramírez, S., Delzenne, N. M., Gomis, R., Claret, M. and Cani, P. D. (2015). *Akkermansia muciniphila* inversely correlates with the onset of inflammation, altered adipose tissue metabolism and metabolic disorders during obesity in mice. Sci. Rep. *5*, 16643.

Schubert, A. M., Sinani, H. and Schloss, P. D. (2015). Antibiotic-induced alterations of the murine gut microbiota and subsequent effects on colonization resistance against *Clostridium difficile*. MBio. Edited by C. M. Fraser *6*, e00974-15.

Seekatz, A. M., Aas, J., Gessert, C. E., Rubin, T. A., Saman, D. M., Bakken, J. S. and Young, V. B. (2014). Recovery of the gut microbiome following fecal microbiota transplantation. MBio *5*, 1–9.

Segura Munoz, R. R., Quach, T., Gomes-Neto, J. C., Xian, Y., Pena, P. A., Weier, S., Pellizzon, M. A., Kittana, H., Cody, L. A., Geis, A. L., et al. (2020). Stearidonic-enriched soybean oil modulates obesity, glucose metabolism, and fatty acid profiles independently of *Akkermansia muciniphila*. Mol. Nutr. Food Res. *64*, 2000162.

Shin, N.-R., Lee, J.-C., Lee, H.-Y., Kim, M.-S., Whon, T. W., Lee, M.-S. and Bae, J.-W. (2014). An increase in the *Akkermansia* spp. population induced by metformin treatment improves glucose homeostasis in diet-induced obese mice. Gut *63*, 727–35.

Smillie, C. S., Sauk, J., Gevers, D., Friedman, J., Sung, J., Youngster, I., Hohmann, E. L., Staley, C., Khoruts, A., Sadowsky, M. J., et al. (2018). Strain tracking reveals the determinants of bacterial engraftment in the human gut following fecal microbiota transplantation. Cell Host Microbe *23*, 229–240.

Sonnenburg, J. L. and Bäckhed, F. (2016). Diet–microbiota interactions as moderators of human metabolism. Nature *535*, 56–64.

Stecher, B., Chaffron, S., Käppeli, R., Hapfelmeier, S., Freedrich, S., Weber, T. C., Kirundi, J., Suar, M., McCoy, K. D., von Mering, C., et al. (2010). Like will to like: Abundances of closely related species can predict susceptibility to intestinal colonization by pathogenic and commensal bacteria. PLOS Pathog. *6*, e1000711.

Tessier, P. R., Kim, M.-K., Zhou, W., Xuan, D., Li, C., Ye, M., Nightingale, C. H. and Nicolau, D. P. (2002). Pharmacodynamic assessment of clarithromycin in a murine model of *pneumococcal pneumonia*. Antimicrob. Agents Chemother. *46*, 1425–1434.

Tramontano, M., Andrejev, S., Pruteanu, M., Klünemann, M., Kuhn, M., Galardini, M., Jouhten, P., Zelezniak, A., Zeller, G., Bork, P., et al. (2018). Nutritional preferences of human gut bacteria reveal their metabolic idiosyncrasies. Nat. Microbiol. *3*, 514–522.

Varghese, N. J., Mukherjee, S., Ivanova, N., Konstantinidis, K. T., Mavrommatis, K., Kyrpides, N. C. and Pati, A. (2015). Microbial species delineation using whole genome sequences. Nucleic Acids Res. *43*, 6761–6771.

Vivarelli, S., Salemi, R., Candido, S., Falzone, L., Santagati, M., Stefani, S., Torino, F., Banna, G. L., Tonini, G. and Libra, M. (2019). Gut microbiota and cancer: From pathogenesis to therapy. Cancers (Basel). *11*, 38.

Walker, A. W. and Lawley, T. D. (2013). Therapeutic modulation of intestinal dysbiosis. Pharmacol. Res. *69*, 75–86.

Walter, J. and Ley, R. (2011). The human gut microbiome: Ecology and recent evolutionary changes. Annu. Rev. Microbiol. *65*, 411–429.

Walter, J., Maldonado-Gómez, M. X. and Martínez, I. (2018). To engraft or not to engraft: an ecological framework for gut microbiome modulation with live microbes. Curr. Opin. Biotechnol. *49*, 129–139.

Walters, W. A., Xu, Z. and Knight, R. (2014). Meta-analyses of human gut microbes associated with obesity and IBD. FEBS Lett. *588*, 4223–4233.

Whitaker, W. R., Shepherd, E. S., Sonnenburg, J. L., Whitaker, W. R., Shepherd, E. S. and Sonnenburg, J. L. (2017). Tunable expression tools enable single-cell strain distinction in the gut microbiome resource tunable expression tools enable single-cell strain distinction in the gut microbiome. Cell *169*, 538–538.

Zhai, R., Xue, X., Zhang, L., Yang, X., Zhao, L. and Zhang, C. (2019). Strain-specific anti-inflammatory properties of two *Akkermansia muciniphila* strains on chronic colitis in mice. Front. Cell. Infect. Microbiol. *9*, 239.

Tables

Table 1. Genome-wide average nucleotide identities among the strains utilized in this study

Genome1 Name	Genome2 Name	ANI1->2	ANI2->1	AF1->2	AF2->1
Bacteroides vulgatus ATCC 8482	*Bacteroides vulgatus* RJ2H1	98.68	98.7	75.58	75.59
Bacteroides vulgatus ATCC 8482	*Akkermansia muciniphila* YL44	65.51	65.67	1.05	1.95
Akkermansia muciniphila ATCC BAA-835	*Akkermansia muciniphila* YL44	99.1	99.1	93.37	90.66
Akkermansia muciniphila ATCC BAA-835	*Bacteroides vulgatus* RJ2H1	65.69	65.69	2.05	1.07

Average nucleotide identity (ANI) and Alignment Fraction (AF) are measuring genetic relatedness. ANI1 and AF1 are calculated with Genome 1 as the reference. ANI2 and AF2 are calculated with Genome 2 as the reference.

Table 2. *In vitro* test of antibiotics. TNTC refers to Too Numerous To Count.

Antibiotic	*B. vulgatus* 8482	*B. vulgatus* RJ2H1	*A. muciniphila* BAA-835	*A. muciniphila* YL44
Mix in media (# of colonies in plate)				
BHIym + 10ug/mL Macrolide tylosin tartrate (MTT)	zero	zero	TNTC	TNTC
BHIym + 10ug/mL Clarithromicyn (Cla)	zero	zero	zero	zero
BHIym + 10ug/mL Ampicillin sodium salt (AMP)	zero	zero	zero	zero
BHIym + 10ug/mL each MTT+CLA+AMP	zero	zero	zero	zero
BHIym + 30ug/mL Macrolide tylosin tartrate (MTT)	TNTC	TNTC	zero	zero
BHIym + 30ug/mL Clarithromicyn (CLA)	zero	20	zero	zero
BHIym + 30ug/mL Ampicillin sodium salt (AMP)	zero	zero	zero	zero
BHIym + 30ug/mL each MTT+CLA+AMP	zero	zero	zero	zero
Media w/o abx (positive control)	TNTC	TNTC	TNTC	TNTC
In Disc (mm radius of halo)				
Ampicillin	8	5	15	15
Kanamycin	No Halo	No Halo	No Halo	No Halo
Chloramphenicol	17	15	No Halo	No Halo
Streptomycin	No Halo	No Halo	No Halo	No Halo
Oxythetracyclin	28	23	No Halo	No Halo
Erythromycin	18	18	No Halo	No Halo

Methods

STAR Methods

RESOURCE AVAILABILITY

Lead contact

Further information and request for resources and reagents should be directed to and will be fulfilled by the Lead Contact, Amanda E. Ramer-Tait (aramer-tait2@unl.edu).

Material Availability

This study did not generate new unique reagents.

Data and Code Availability

Original/source data for figures and tables in the paper are available at DOI: 10.17632/gbc76stz42.1.

EXPERIMENTAL MODEL AND SUBJECT DETAILS

Female germ-free C57BL/6 mice were born and reared in flexible film isolators and maintained under gnotobiotic conditions (Temperature 20°C, relative humidity 60%, 14h light/10h dark cycle) at the University of Nebraska-Lincoln. All mice were fed an autoclaved chow diet (LabDiet 5K67, Purina Foods, St. Louis, MO) ad libitum. The Institutional Animal Care and Use Committee at the University of Nebraska-Lincoln approved all procedures involving animals (protocols 1215 and 1700).

METHOD DETAILS

Bacterial cultures

Bacterial strains used in this study were: *Akkermansia muciniphila* BAA-835 (American Tissue Culture Collection, Manassas, VA) isolated from human feces, *A. muciniphila* YL44 (Leibniz Institute DSMZ, Braunschweig, Germany) isolated from C57BL/6J mouse feces, *Bacteroides vulgatus* 8482 (American Tissue Culture Collection), and *B. vulgatus* RJ2H1 (Martínez et al., 2018). *A. muciniphila* strains were cultured in 10 mL Brain Heart Infusion (BHI) medium (BD, Sparks, MD) supplemented with 0.3 % (w/v) mucin (Sigma-Aldrich, St. Louis, MO) and 0.5% yeast extract (BD, Sparks, MD); this medium is referred to as BHIm in this manuscript. *B. vulgatus* strains were grown in 10 mL BHI medium supplemented with menadione (0.001 g/L, Sigma-Aldrich), hemin (0.005 g/L, Sigma-Aldrich), and an additional 0.5% yeast extract (BD, Sparks, MD); this medium is referred to as BHIs throughout this manuscript.

To inoculate mice, one vial of each bacterial strain was retrieved from -80°C storage and the entire contents were struck onto a plate containing BHIm with agar (1% w/v). Plates were incubated at 37°C under anaerobic conditions for either three days for *B. vulgatus* strains or five days for *A. muciniphila* strains. Colonies were then transferred into 30 mL BHIm or BHIs and incubated anaerobically at 37°C. After 24 hr, 300 µL of each culture was transferred into a fresh 30 mL of BHIm or BHIs. After 18 hr, these

cultures were centrifuged (3000 x g for 15 min), resuspended in 1X PBS (HyClone, Logan, UT) to achieve a concentration of 1.0 x 10^9 CFU/mL, and administered to mice via oral gavage (100 µL/mouse). For some experiments, *A. muciniphila* BAA-835 and *B. vulgatus* ATCC 8482 were prepared as described above and then mixed together in a 1:1 ratio prior to administering to mice (100 µL/mouse). A mixture containing both *A. muciniphila* YL44 and *B. vulgatus* RJ2H1 was also prepared for mice in this manner.

Gnotobiotic mice with complex microbiomes

Mouse cecal contents from a C57BL/6J mouse population housed at Max F. Perutz Laboratories in Austria were used as the positive microbiome for our studies as it naturally harbored both *A. muciniphila* and *B. vulgatus* (previously referred to as MFBL) (Lagkouvardos et al., 2016). Cecal contents from a wild mouse population in the Massif Central region of France previously maintained at the Max Planck Institute for Evolutionary Biology (Plon, Germany) were used as the negative microbiome for our studies as it was naturally deficient in both *A. muciniphila* and *B. vulgatus* (previously referred to as A (Martínez et al., 2018) and MC608-F-a1 (Lagkouvardos et al., 2016)). The presence and absence of *A. muciniphila* and *B. vulgatus* in both microbiomes was confirmed based on previous 16S rRNA gene sequencing results (Martínez et al., 2018) and species-specific qPCR (Segura Munoz et al., 2020). To produce sufficient and standardized inocula for all studies, germ-free C57BL/6 mice were colonized with cecal contents from the donor mice and maintained under gnotobiotic conditions at the University of Nebraska-Lincoln for four weeks. Ceca were then collected, stored at -80°C, and the contents resuspended (1:10 wt/vol) in reduced PBS as previously described (Bindels et al., 2017) at the time of use.

Mice

Female germ-free C57BL/6 mice were born and reared in flexible film isolators and maintained under gnotobiotic conditions at the University of Nebraska-Lincoln. At six weeks of age, mice were transferred from isolators to an individually ventilated cage (IVC) system, housed four to five mice per cage, and maintained as previously described (Gomes-Neto, Mantz, et al., 2017). Within three hours after transfer to the IVC system, mice were colonized with the respective microbiomes described above via oral gavage (100 µL/mouse). All mice were fed an autoclaved chow diet (LabDiet 5K67, Purina Foods, St. Louis, MO) ad libitum. The Institutional Animal Care and Use Committee at the University of Nebraska-Lincoln approved all procedures involving animals (protocols 1215 and 1700).

Tests of persistence, coexistence, and the importance of colonization order

To determine to what degree the colonization dynamics of *A. muciniphila* and *B. vulgatus* strains were influenced by the presence or absence of the respective species present in the gut microbiome, germ-free

mice were colonized with a microbiome identified as either positive or negative for *A. muciniphila* and *B. vulgatus* (week 0). Two weeks later (week 2), these mice were administered either a mixture of *A. muciniphila* BAA-835 and *B. vulgatus* 8482 or a mixture of *A. muciniphila* YL44 and *B. vulgatus* RJ2H1 for a total of two treatments. Each treatment consisted of five mice housed in one cage, and fecal samples were collected weekly at weeks 1, 2, 3, 4, 5, 6, and 7.

To test if colonization could be blocked or influenced by introducing one strain into the gut ecosystem before the other, germ-free mice were orally gavaged (week 0) with a negative microbiome (devoid of *A. muciniphila* and *B. vulgatus*) and a mixture of *A. muciniphila* BAA-835 and *B. vulgatus* 8482. Two weeks later (week 2), mice were orally gavaged with strains YL44 and RJ2H1. In a separate experiment, the importance of colonization order was tested by inverting the order of strain introduction. Specifically, GF mice were orally gavaged (week 0) with a negative microbiome and a mixture of either *A. muciniphila* YL44 and *B. vulgatus* RJ2H1. Two weeks later (week 2), mice were orally gavaged with strains BAA-835 and 8482. Studies were also performed to test the relative fitness of *A. muciniphila* and *B. vulgatus* strains when introduced at the same time. Germ-free mice were colonized with the negative microbiome at week 0 and then administered a mixture of all four strains at week 2. For all studies, each treatment consisted of five mice housed in one cage, and fecal samples were collected weekly at weeks 1, 2, 3, 4, 5, 6, and 7.

Quantitative real-time PCR (qPCR)

Strain-specific primers were designed to target unique genes (identified using IMG-ER, Joint Genome Institute) (Chen et al., 2019) present in each strain but absent in other strains, including those used here as well as all available *A. muciniphila* or *B. vulgatus* sequences reported in the NCBI GOLD database (Mukherjee et al., 2018). Once unique genes were identified, specific primer pairs were generated using Prime3 software (Rozen et al., 2000) and their quality assessed with NetPrimer (Premier Biosoft, San Francisco, CA). Strain-specific primers designed for this study are listed in Key Resources. Thermocycling conditions for all four strain-specific primer pairs were: (i) initial denaturation step at 95°C for 5 min; (ii) 35 cycles of 95°C for 1 min, 64.2°C for 30 sec, 72°C for 30 sec; and (iii) one 20-min interval to generate a melting curve by progressively increasing the temperature from 60°C to 95°C.

Species-specific primers for *B. vulgatus* were also designed using a similar approach as for the strain-specific primers where primers targeted unique genes that were present in this species but absent in all other bacterial sequences reported in NCBI. The species-specific primers targeting *B. vulgatus* are listed in Key Resources. Previously published species-specific primers were used to quantify *A. muciniphila.* (Schneeberger et al., 2015). Thermocycling conditions for both *B. vulgatus* and *A. muciniphila* species-specific primer pairs were: (i) initial denaturation step at 95°C for 5 min; (ii) 35 cycles of 95°C for 1 min, 57°C for 45 sec, and 72°C for 45 sec; and (iii) one 20-min interval to generate a melting curve by progressively increasing the temperature from 60°C to 95°C.

All qPCRs were performed using SYBR green (Thermo Scientific, Lithuania) and a Mastercycler Realplex2 (Eppendorf AG, Hamburg, Germany). Specificity was tested using DNA from the strain of interest and the negative microbiomes utilized in this study. Optimal thermocycling conditions for qPCR were determined via gradient PCR using twelve temperatures between 53°C and 63°C (equal intervals) (Gomes-Neto, Mantz, et al., 2017).

To make qPCR standard curves, aliquots of duplicate log-phase *A. muciniphila* or *B. vulgatus* cultures were plated on either BHIs or BHIm media for quantification of colony forming units per milliliter of culture (CFU/mL). A phenol chloroform method (Gomes-Neto, Kittana, et al., 2017) was used for DNA extraction. Quantitative PCR including melt curve analysis, was performed on serially diluted (ten-fold) extracted DNA. Bacterial abundance was calculated based on the linear relationship between fluorescence of serially diluted DNA and corresponding CFU/mL (Gomes-Neto, Mantz, et al., 2017). Minimum limit of detection was established to be the lowest DNA dilution at which the relationship between CFU and fluorescence was linear.

Genomic analyses

IMG/MER tools (Mukherjee et al., 2018; Chen et al., 2019) from the Joint Genome Institute were used to calculate genome-wide average nucleotide identity (gANI) and alignment fractions (AF) as previously described (Varghese et al., 2015). Genome size information from strains reported at NCBI was used to generate histogram distribution using the ggplot2 package in RStudio (RStudio Team, Boston, MA). The IMG/MER phylogenetic profiler tool was used to perform gene context analysis and identify unique genes and protein families (pfam) for each strain (Mavromatis et al., 2009; Mukherjee et al., 2018; Chen et al., 2019). Classifications of identified protein families were made based on descriptions in the protein family database (El-Gebali et al., 2019) and the Universal Protein Resource (Consortium, 2008). Pie charts and stacked bar graphs were create using Prism 8 (GraphPad Software, San Diego, CA).

Tests for antibiotic sensitivity

To determine sensitivity of *Akkermansia* strains to antibiotics *in vitro*, BHIm agar plates containing multiple combinations of ampicillin (AMP), microlide Tylosine tartrate (MTT), and clarithromycin (CLA) were prepared. A set of BHIm and BHIs agar plates prepared without antibiotics were used as a control. A 500 µL aliquot of each strain was spread to create a lawn; plates were then incubated as described above and monitored for the presence/absence of CFUs. The sensitivity of *A. muciniphila* strains to additional antibiotics (Table 2) was evaluated via disk diffusion tests using a second set of BHIm and BHIs agar plates prepared without antibiotics (Brown et al., 1975).

Subtractive microbiome modulation in mice using antibiotics

Germ-free mice were gavaged with the negative microbiome and *A. muciniphila* BAA-835 (day -7). One week later (day 0), mice were either left untreated (control) or given one of the following five antibiotic treatments for five days: MTT, CLA, AMP, AMP + MTT, or AMP + MTT + CLA. Antibiotic treatments containing AMP and/or MTT were administered via the drinking water at 1.33 mg/mL and 1 mg/mL, respectively (Livanos et al., 2016). Antibiotics in the drinking water were replaced daily during the five-day treatment period. Because CLA has low solubility in water, CLA was suspended at 1 mg/mL in a 1:5 solution of dimethyl sulfoxide (Sigma-Aldrich) and water (Tessier et al., 2002) and then orally gavaged daily to mice for five days (100uL/mouse) (Tessier et al., 2002). Cages were changed daily during the antibiotic treatment period to limit recolonization through coprophagy. Each treatment consisted of three to six mice housed two to five per cage. Fecal samples were collected prior to the introduction of antibiotics (day 0) and on days 3 and 5 during antibiotic treatment. On day 5 (after the fecal collection), all antibiotic solutions were replaced with regular drinking water. Mice were orally gavaged with *A. muciniphila* YL44 (3×10^8 CFU/mL) daily for five days, and fecal samples were collected on day 10 after last YL44 gavage and then weekly for 5 weeks.

QUANTIFICATION AND STATISTICAL ANALYSIS

All longitudinal data were analyzed using two-way ANOVA repeated measures and Tukey test multiple pairwise comparisons using Prism 8 (GraphPad Software). A *p*-value of 0.05 was considered significant.

KEY RESOURCES TABLE

REAGENT or RESOURCE	SOURCE	IDENTIFIER
Bacterial and Virus Strains		
Akkermansia muciniphila ATCC BAA-835	www.atcc.org	ATCC BAA-835
Akkermansia muciniphila YL44	www.dsmz.de	YL44
Bacteroides vulgatus ATCC 8482	www.atcc.org	ATCC 8482
Bacteroides vulgatus RJ2H1	Martinez et al, 2018	RJ2H1
Biological Samples		
Fecal samples	This study	N/A
Positive microbiome	Lagkouvardos et al., 2016	MFBL
Negative microbiome	Lagkouvardos et al., 2016	MC608-F-a1
Chemicals, Peptides, and Recombinant Proteins		
Phenol Chloroform / Isoamyl Alcohol	Acros Organics	327115000
Lyzosyme	MP Biomedicals	100831
Triton-X 100	Fisher	BP151
Proteinase K	Qiagen	1114886
Ampicillin	Sigma-Aldrich	A9518
Microlide Tylosin Tartrate	Alfa Aesar	J62633
Clarithromycin	Alfa Aesar	J66055
Brain Heart Infusion	BD Biosciences	211059
Mucin from porcine stomach Type II	Sigma-Aldrich	M1778
Critical Commercial Assays		
SYBRgreen master mix	Thermo Scientific	K0253
Deposited Data		
All data	DOI: 10.17632/gbc76stz42.1	
Experimental Models: Organisms/Strains		
Mus musculus domesticus C57BL/6 female	Nebraska Gnotobiotic Mouse Program	C57BL/6 female
Oligonucleotides		
Primer: *A. muciniphila* Forward: CAGCACGTGAAGGTGGGGAC	Schneeberger et al., 2015	N/A

Primer: *A. muciniphil*a Reverse: CCTTGCGGTTGGCTTCAGAT	Schneeberger et al., 2015	N/A
Primer: *B. vulgatus* Forward: GGCAGCATGGTCTTAGCTTGC	This paper	N/A
Primer: *B. vulgatus* Reverse: GTGAACATGCGGACTCATGATG	This paper	N/A
Primer: *A. muciniphila* BAA-835 Forward: CGGGGACAGTATATCGGGGA	This paper	N/A
Primer: *A. muciniphila* BAA-835 Reverse: GAGATTCGGATAGCGCACCA	This paper	N/A
Primer: *A. muciniphila* YL44 Forward: GCCTTTCTTCAGCAAACGGG	This paper	N/A
Primer: *A. muciniphila* YL44 Reverse: TCACAGCAGTTCAACAGGCA	This paper	N/A
Primer: *B. vulgatus* 8482 Forward: TCATCGTGGTCCATTGTCGG	This paper	N/A
Primer: *B. vulgatus* 8482 Reverse: AACACCCCGTCAAAATTGCG	This paper	N/A
Primer: *B. vulgatus* RJ2H1 Forward: GCCGACGCTTTCTGACAAAA	This paper	N/A
Primer: *B. vulgatus* RJ2H1 Reverse: GAGGCGGCTTTCCATTGTTC	This paper	N/A
Software and Algorithms		
Prism 8	GraphPad Software, San Diego, CA.	Version 8
IMG/MER	Joint Genome Institute	N/A
Prime3 software	Reference 40	N/A
NetPrimer	Premier Biosoft, San Francisco, CA	N/A
RStudio: Integrated Development for R	RStudio Team, Boston, MA	N/A
Other		

Figures

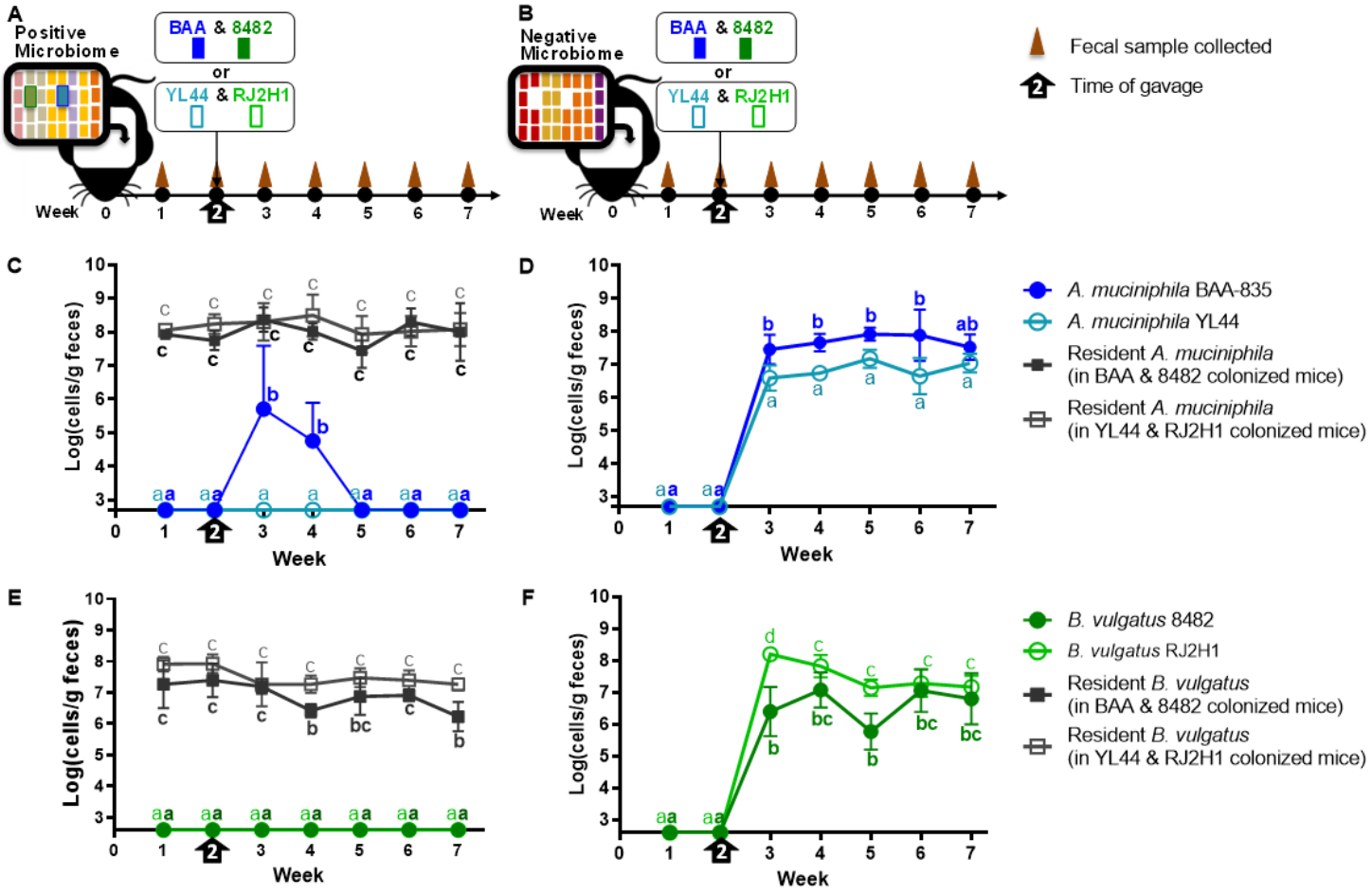

Figure 1

A. muciniphila and B. vulgatus strains only colonized gnotobiotic mice harboring complex microbiomes devoid of exactly these species. Experimental design to test colonization of strains in mice harboring a microbiome with (positive; A) and without (negative; B) A. muciniphila and B. vulgatus (B). Brown triangles represent timepoints for fecal sample collections. Black arrow represents colonization with A. muciniphila and B. vulgatus strains at week 2. Week 2 fecal samples were collected prior to inoculating with test strains. Abundance of A. muciniphila species (gray), strain BAA-835 (dark blue), and strain YL44 (light blue) in mice harboring either a positive (C) or a negative (D) microbiome. Abundance of B. vulgatus species (gray), strain 8482 (dark green), and strain RJ2H1 (light green) in mice harboring either a positive (E) or a negative (F) microbiome. Values are presented as mean + the standard deviation. Time points with different letters are significantly ($p<0.05$) different from one another at indicated timepoints by two-way ANOVA repeated measures and Tukey test multiple pairwise comparisons in each plot.

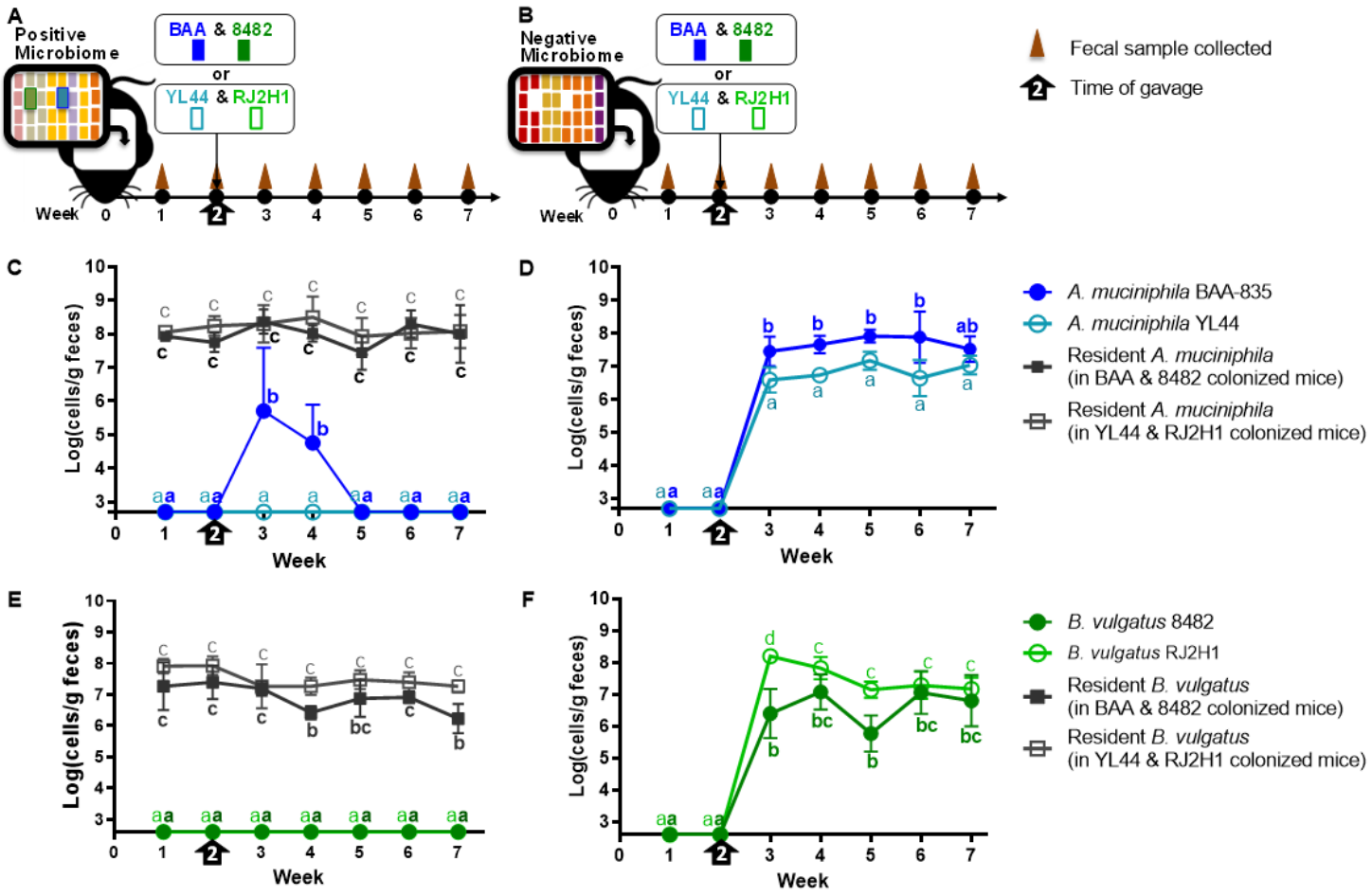

Figure 1

A. muciniphila and B. vulgatus strains only colonized gnotobiotic mice harboring complex microbiomes devoid of exactly these species. Experimental design to test colonization of strains in mice harboring a microbiome with (positive; A) and without (negative; B) A. muciniphila and B. vulgatus (B). Brown triangles represent timepoints for fecal sample collections. Black arrow represents colonization with A. muciniphila and B. vulgatus strains at week 2. Week 2 fecal samples were collected prior to inoculating with test strains. Abundance of A. muciniphila species (gray), strain BAA-835 (dark blue), and strain YL44 (light blue) in mice harboring either a positive (C) or a negative (D) microbiome. Abundance of B. vulgatus species (gray), strain 8482 (dark green), and strain RJ2H1 (light green) in mice harboring either a positive (E) or a negative (F) microbiome. Values are presented as mean + the standard deviation. Time points with different letters are significantly ($p<0.05$) different from one another at indicated timepoints by two-way ANOVA repeated measures and Tukey test multiple pairwise comparisons in each plot.

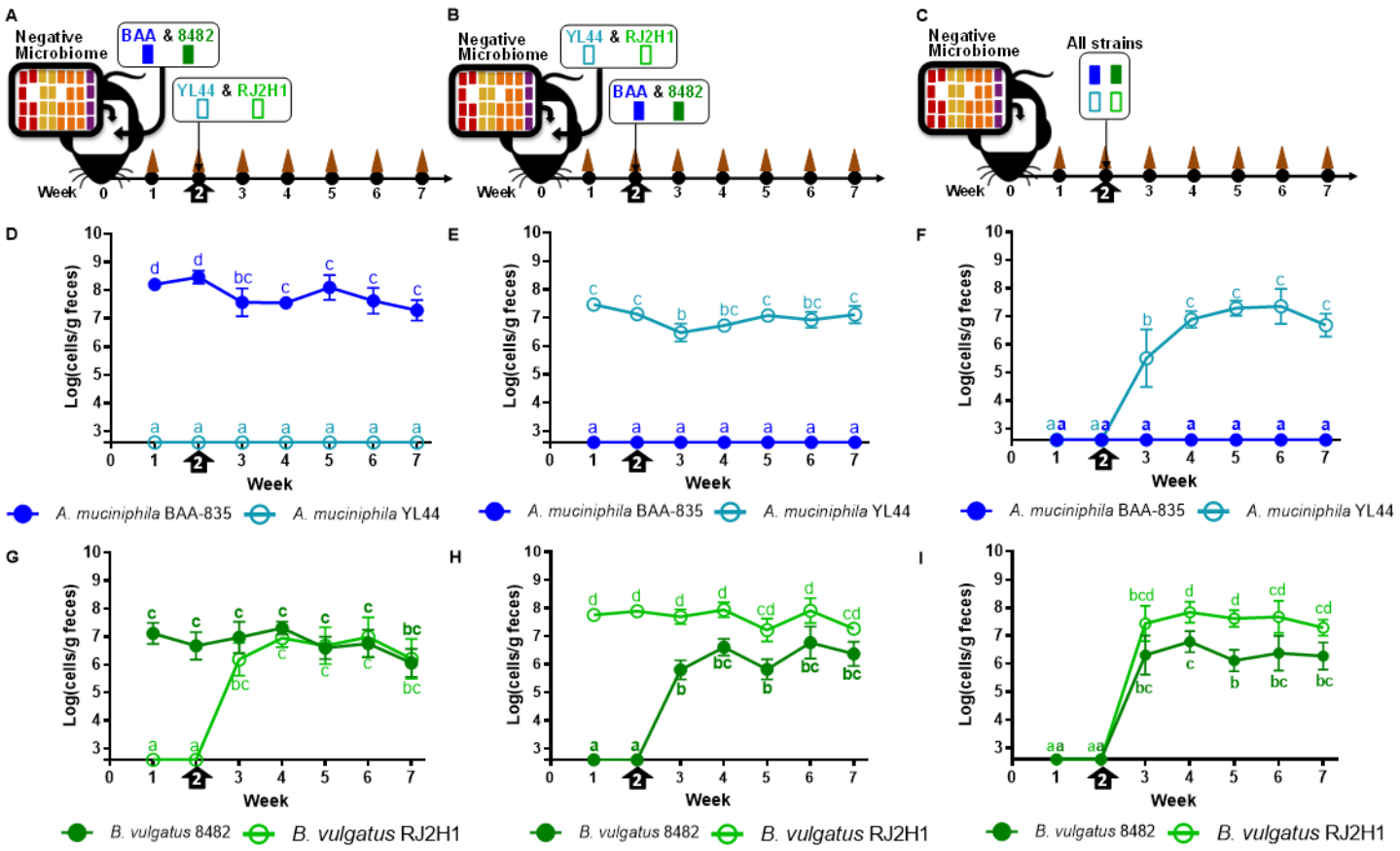

Figure 2

Colonization of A. muciniphila, but not B. vulgatus, was strictly governed by competitive exclusion and priority effects. All mice were colonized at week 0 with a negative microbiome devoid of A. muciniphila and B. vulgatus. Competition experiments with strains of A. muciniphila and B. vulgatus were performed as follows: (A, D, G) A. muciniphila BAA-835 and B. vulgatus 8482 were introduced at week 0 prior to introduction of A. muciniphila YL44 and B. vulgatus RJ2H1 at week 2. (B, E, H) A. muciniphila YL44 and B. vulgatus RJ2H1 were introduced at week 0 prior to introduction of A. muciniphila BAA-835 and B. vulgatus 8482 at week 2. (C, F, I) A. muciniphila and B. vulgatus strains were all introduced into mice at the same time. (D-F) Abundance of A. muciniphila strain BAA-835 (dark blue) and strain YL44 (light blue) in feces. (G-I) Abundance of B. vulgatus strain 8482 (dark green) and strain RJ2H1 (light green) in feces. Week 2 fecal samples were collected prior to inoculating with test strains. Values are presented as mean + the standard deviation. Time points with different letters are significantly ($p<0.05$) different from one another by two-way ANOVA repeated measures and Tukey test multiple pairwise comparisons among treatments of A. muciniphila (D-F) or B. vulgatus (G-I).

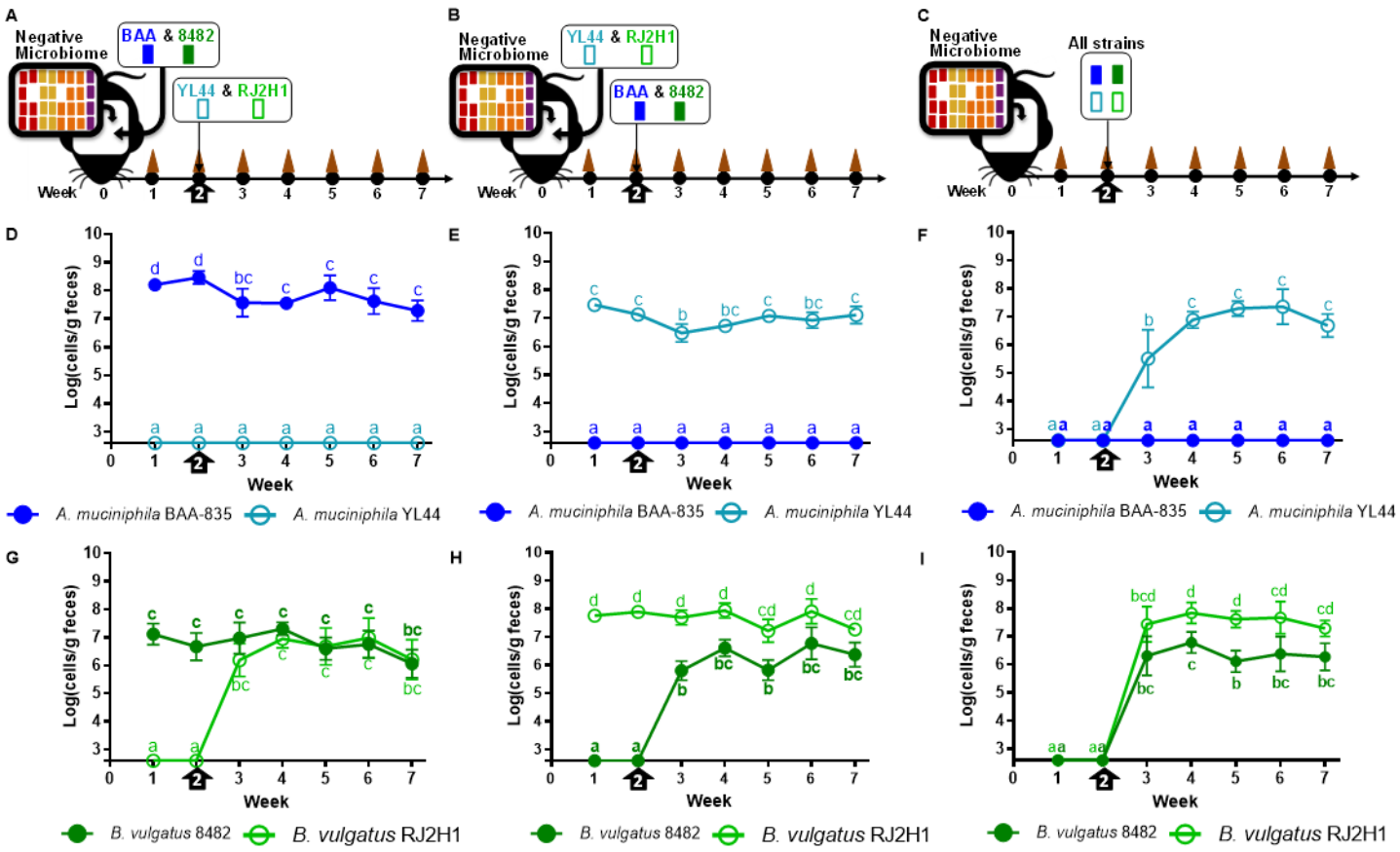

Figure 2

Colonization of A. muciniphila, but not B. vulgatus, was strictly governed by competitive exclusion and priority effects. All mice were colonized at week 0 with a negative microbiome devoid of A. muciniphila and B. vulgatus. Competition experiments with strains of A. muciniphila and B. vulgatus were performed as follows: (A, D, G) A. muciniphila BAA-835 and B. vulgatus 8482 were introduced at week 0 prior to introduction of A. muciniphila YL44 and B. vulgatus RJ2H1 at week 2. (B, E, H) A. muciniphila YL44 and B. vulgatus RJ2H1 were introduced at week 0 prior to introduction of A. muciniphila BAA-835 and B. vulgatus 8482 at week 2. (C, F, I) A. muciniphila and B. vulgatus strains were all introduced into mice at the same time. (D-F) Abundance of A. muciniphila strain BAA-835 (dark blue) and strain YL44 (light blue) in feces. (G-I) Abundance of B. vulgatus strain 8482 (dark green) and strain RJ2H1 (light green) in feces. Week 2 fecal samples were collected prior to inoculating with test strains. Values are presented as mean + the standard deviation. Time points with different letters are significantly ($p<0.05$) different from one another by two-way ANOVA repeated measures and Tukey test multiple pairwise comparisons among treatments of A. muciniphila (D-F) or B. vulgatus (G-I).

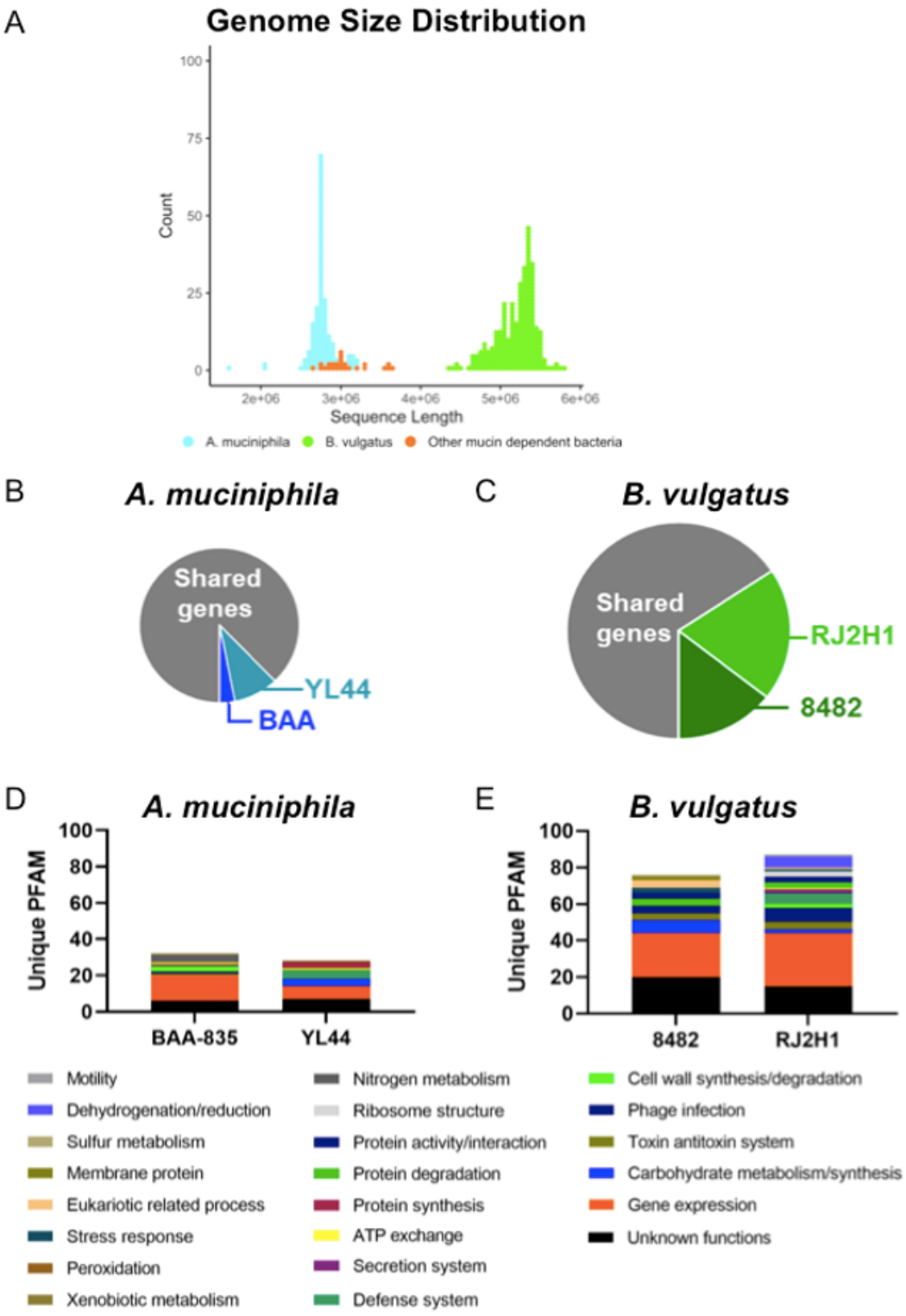

Figure 3

Genomic differences between A. muciniphila and B. vulgatus strains. (A) Shared (gray) and unique genes for A. muciniphila BAA-835 (dark blue) and YL44 (light blue). (B) Shared (gray) and unique genes for B. vulgatus 8482 (dark green) and RJ2H1 (light green). Sizes of pie charts are scaled to represent proportional differences between A. muciniphila and B. vulgatus genomes. Biological processes related

to unique protein families are depicted for A. muciniphila (C) and B. vulgatus (D) strains. Each protein is grouped by colors that represent an individual biological process.

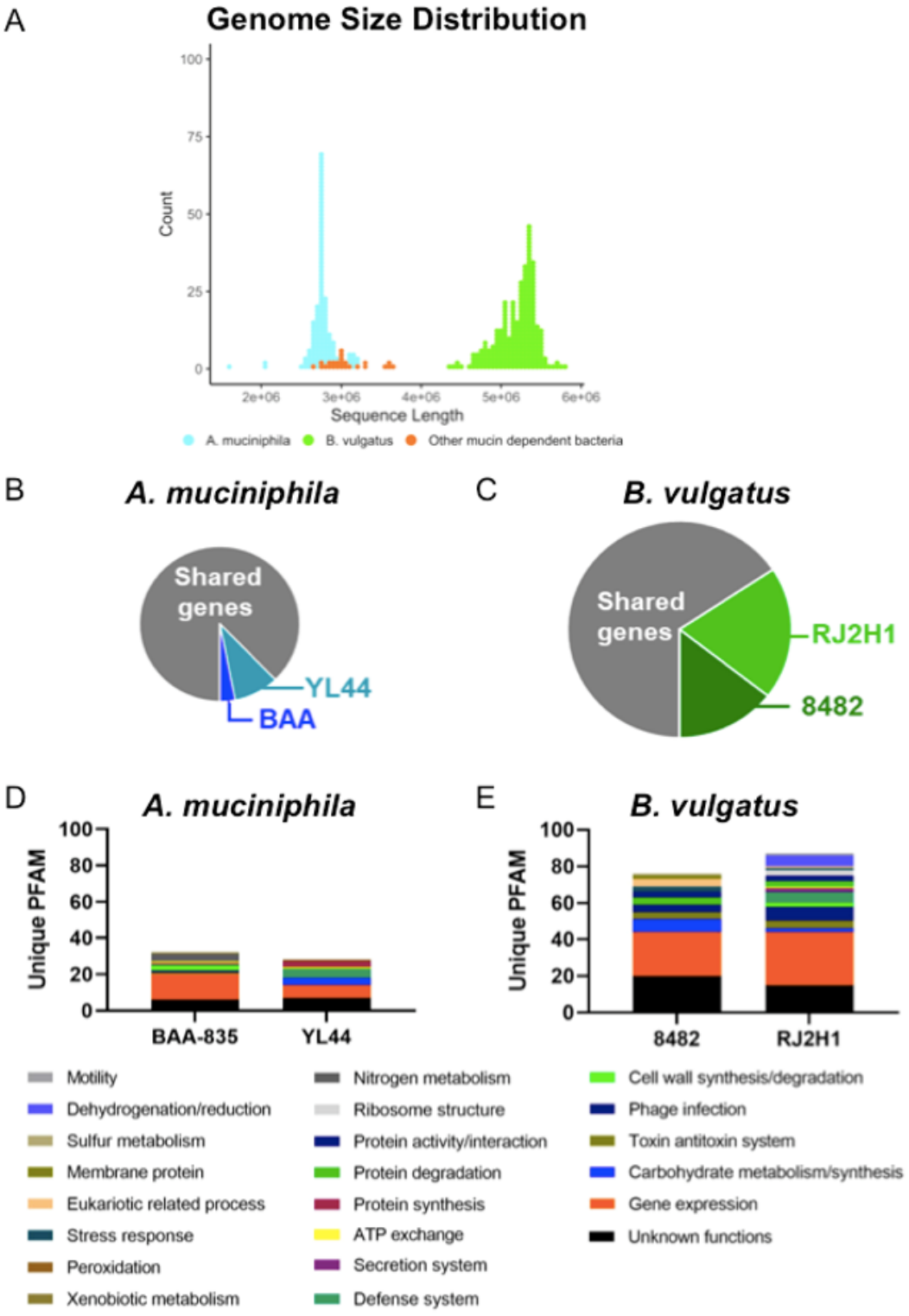

Figure 3

Genomic differences between A. muciniphila and B. vulgatus strains. (A) Shared (gray) and unique genes for A. muciniphila BAA-835 (dark blue) and YL44 (light blue). (B) Shared (gray) and unique genes for B. vulgatus 8482 (dark green) and RJ2H1 (light green). Sizes of pie charts are scaled to represent

proportional differences between A. muciniphila and B. vulgatus genomes. Biological processes related to unique protein families are depicted for A. muciniphila (C) and B. vulgatus (D) strains. Each protein is grouped by colors that represent an individual biological process.

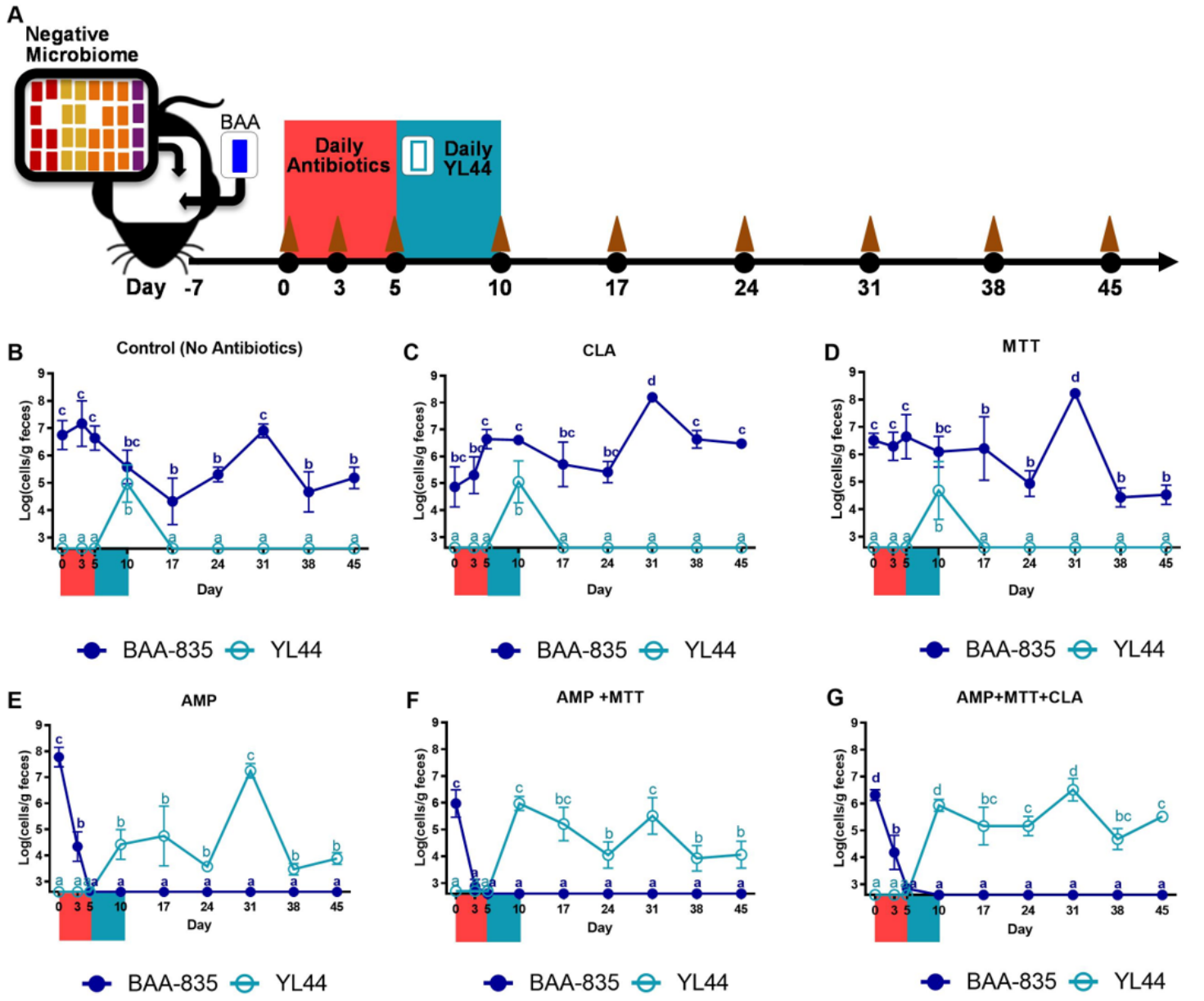

Figure 4

A subtractive antibiotic strategy enabled replacement of an established A. muciniphila strain. (A) Experimental design depicting conventionalization of germ-free mice with a negative microbiota devoid of A. muciniphila and colonization with strain BAA-835 at day -7. On day 0, mice were treated with antibiotics for five days. On day 5, mice receiving antibiotics were returned to regular drinking water and fecal samples were collected. Also on day 5, mice began receiving daily gavages of YL44 for five days. Brown triangles represent timepoints for fecal sample collections. Abundance of A. muciniphila BAA-835 (dark blue) and A. muciniphila YL44 (light blue) in feces of mice not treated with antibiotics (B) or treated with CLA alone (C), MTT alone (D), AMP alone (E), AMP + MTT (F), or AMP + MTT + CLA (G). Values are

presented as mean + the standard deviation. In each plot, time points with different letters are significantly ($p<0.05$) different from one another by two-way ANOVA repeated measures and Tukey test multiple pairwise comparisons.

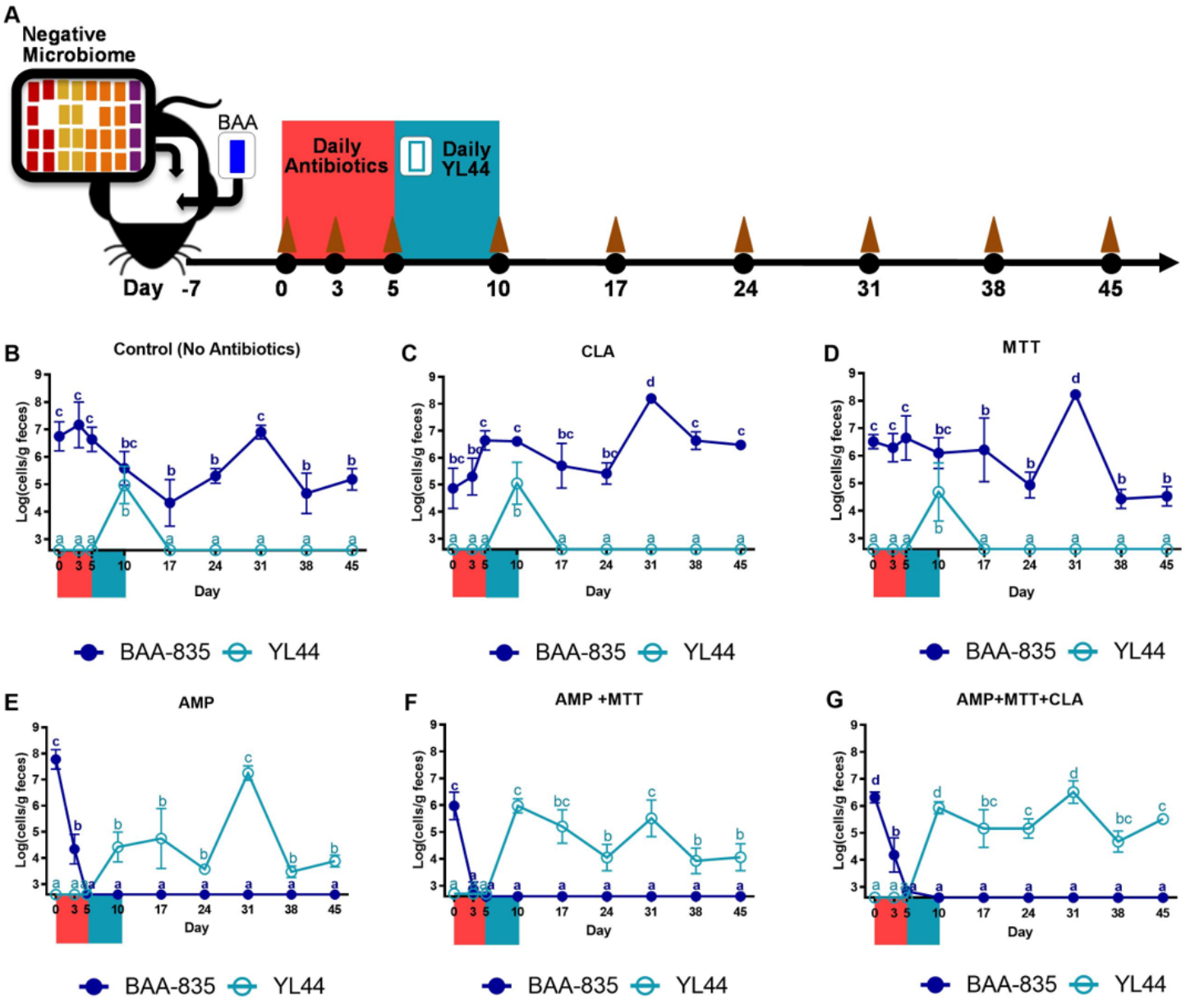

Figure 4

A subtractive antibiotic strategy enabled replacement of an established A. muciniphila strain. (A) Experimental design depicting conventionalization of germ-free mice with a negative microbiota devoid of A. muciniphila and colonization with strain BAA-835 at day -7. On day 0, mice were treated with antibiotics for five days. On day 5, mice receiving antibiotics were returned to regular drinking water and fecal samples were collected. Also on day 5, mice began receiving daily gavages of YL44 for five days. Brown triangles represent timepoints for fecal sample collections. Abundance of A. muciniphila BAA-835 (dark blue) and A. muciniphila YL44 (light blue) in feces of mice not treated with antibiotics (B) or treated with CLA alone (C), MTT alone (D), AMP alone (E), AMP + MTT (F), or AMP + MTT + CLA (G). Values are

presented as mean + the standard deviation. In each plot, time points with different letters are significantly ($p<0.05$) different from one another by two-way ANOVA repeated measures and Tukey test multiple pairwise comparisons.